

Chemical Factors that Control Lignin Polymerization

Amandeep K. Sangha,[†] Brian H. Davison,^{‡,§} Robert F. Standaert,^{§,#,||} Mark F. Davis,[⊥] Jeremy C. Smith,^{†,‡,#} and Jerry M. Parks^{*,†,‡,§}

[†]UT/ORNL Center for Molecular Biophysics, Oak Ridge National Laboratory, Oak Ridge, Tennessee 37831-6309, United States

[‡]Bioenergy Science Center, [§]Biosciences Division, and ^{||}Biology and Soft Matter Division, Oak Ridge National Laboratory, Oak Ridge, Tennessee 37831, United States

[⊥]National Bioenergy Center and Bioenergy Science Center, National Renewable Energy Laboratory, Golden, Colorado 80401, United States

[#]Department of Biochemistry and Cellular and Molecular Biology, University of Tennessee, Knoxville, Tennessee 37996, United States

S Supporting Information

ABSTRACT: Lignin is a complex, branched polymer that reinforces plant tissue. Understanding the factors that govern lignin structure is of central importance to the development of technologies for converting lignocellulosic biomass into fuels because lignin imparts resistance to chemical, enzymatic, and mechanical deconstruction. Lignin is formed by enzymatic oxidation of phenolic monomers (monolignols) of three main types, guaiacyl (G), syringyl (S), and *p*-hydroxyphenyl (H) subunits. It is known that increasing the relative abundance of H subunits results in lower molecular weight lignin polymers and hence more easily deconstructed biomass, but it is not known why. Here, we report an analysis of frontier molecular orbitals in mono-, di-, and trilignols, calculated using density functional theory, which points to a requirement of strong *p*-electron density on the reacting phenolic oxygen atom of the neutral precursor for enzymatic oxidation to occur. This model is consistent with a proton-coupled electron transfer (PCET) mechanism and for the first time explains why H subunits in certain linkages (β - β or β -5) react poorly and tend to “cap” the polymer. In general, β -5 linkages with either a G or H terminus are predicted to inhibit elongation. More broadly, the model correctly accounts for the reactivity of the phenolic groups in a diverse set of dilignols comprising H and G subunits. Thus, we provide a coherent framework for understanding the propensity toward growth or termination of different terminal subunits in lignin.



INTRODUCTION

Lignin is the second most abundant biopolymer, after cellulose, on earth. Found in plant cell walls, lignin provides mechanical strength to plant stems, supports the flow of water through the xylem, and provides defense against chemical and microbial attack of the cell wall. Conversion of lignocellulosic biomass into biofuels has attracted much attention due to its potential to reduce fossil fuel dependence.^{1,2} Nonfood crops, such as grasses and poplar, provide sustainable raw materials for the biofuel industry. However, due to its interactions with cellulose, hemicellulose, and other cell wall matrix components, lignin forms physical barriers to enzymatic accessibility of polysaccharides³ and is a major contributor to biomass recalcitrance.^{4,5} Physical, chemical, or biological pretreatment is used to detach lignin from biomass and make the fermentable sugars more accessible.^{6–11} Pretreatment poses a challenge to biofuel production at commercial levels due to its high cost.^{4,5,12} Genetically engineered plants with modified lignin content and composition have been shown to improve lignin extractability and increase saccharide yield.¹³

To make further improvements on a rational basis, understanding the factors that control the composition and structure of lignin is needed. Lignin is a complex, heterogeneous material made primarily of three phenylpropanoid precursors, *p*-coumaryl, coniferyl, and sinapyl alcohols, also known as monolignols (Figure 1). When incorporated into lignin, these constituents are referred to as *p*-hydroxyphenyl (H), guaiacyl (G), and sinapyl (S) subunits, respectively. The composition of lignin, that is, the relative abundance of H, G, and S subunits, varies by species, cell or tissue type, and age.^{14,15} The complex structural and chemical properties of the lignin polymer lead to its resistance toward degradation.

It has been shown that increasing the H content of lignin in *Medicago sativa* (alfalfa) by down-regulating *p*-coumarate 3-hydroxylase (C3H) or hydroxycinnamoyl-CoA/shikimate hydroxycinnamoyltransferase (HCT) leads to lignin with

Received: December 7, 2013

Revised: December 16, 2013

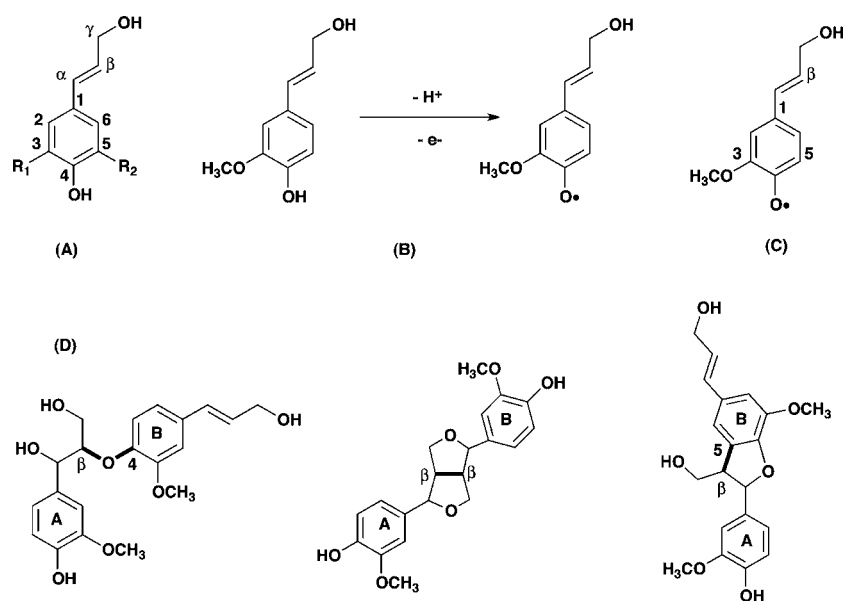


Figure 1. (A) Atom numbering for the phenylpropanoid unit in monolignols. For *p*-coumaryl, $R_1, R_2 = H$; coniferyl, $R_1 = H, R_2 = OCH_3$; sinapyl, $R_1, R_2 = OCH_3$. (B) Oxidation of a phenylpropanoid yields a phenol radical. (C) Radical delocalization leads to additional reactive sites at C1, C3, C5, and $C\beta$. (D) Examples of common linkages found in natural lignin: (left to right) β -O4 (β -aryl ether), β - β (resinol), and β -5 (phenylcoumaran).

lower molecular weight, the practical consequence of which is improved polysaccharide release.¹⁶ It is therefore intriguing to ask why increasing the H-lignin content leads to the observed reduction in the degree of polymerization. One possibility is that H subunits bind more poorly than G and S subunits in the active sites of enzymes involved in radical formation. Another hypothesis, investigated here, is that the three types of subunits have intrinsic chemical differences that govern the rates of formation and reaction of the derived phenolic radicals.

The mechanism of lignin polymerization is not completely understood,¹⁷ but the overall process involves endwise polymerization in which phenolic radicals formed from oxidation of the monolignols undergo coupling reactions with analogous radicals formed on growing lignin chains (Figure 1B).^{18–22} *In vitro* and *in vivo*, the oxidation is catalyzed by peroxidases and laccases,^{23–25} but polymerization can also be affected by nonenzymatic oxidation. Besides being reactive at their phenolic oxygens, the monolignol-derived radicals are reactive at C1, C3, C5, and C8 ($C\beta$) due to delocalization of spin throughout the conjugated π system (Figure 1C), although steric hindrance often limits or precludes reactivity at some of those sites.²⁶ The presence of multiple reactive sites leads to a large number of permutations in coupling reactions that yield numerous possible interunit bonds. The most common of these found in natural lignin are β -O4, β - β , and β -5 bonds (Figure 1D),²⁰ and quantum chemical calculations have shown that their formation from pairs of monolignol radicals is enthalpically more favorable than that for other, less common interunit linkages.²⁷

In this work, we investigated how specific interunit linkages in a series of model di- and trilignols comprising *p*-hydroxyphenyl (H) and guaiacyl (G) subunits linked by the common β -O4, β - β , and β -5 linkages affect the favorability of oxidation and subsequent reaction of terminal phenolic groups required for chain elongation. To address these two issues, we used density functional theory first to calculate bond dissociation energies (BDEs) for the parent phenolic compounds and then to perform frontier molecular orbital

(MO) analyses. The results of these calculations were considered in light of a prior electron paramagnetic resonance (EPR)-based study of horseradish peroxidase (HRP)-mediated oxidative dehydrogenation of monolignols and several dilignols.²⁸ From our analysis, we concluded that the BDE, while important, is alone a poor predictor for the observed patterns of reactivity. Rather, reactivity is better predicted by the combination of MO energy and electron density on the phenolic oxygen in the neutral lignin precursors. Using this approach, we were able to rationalize the experimental observations on the ability, or lack thereof, of lignin precursors to undergo radical formation and participate in endwise polymerization. Our results thus indicate that the reduced capacity of H subunits for endwise polymerization can be explained by intrinsic chemical factors.

COMPUTATIONAL DETAILS

In phenolic radical coupling, the initial products are often unstable and quickly undergo further reactions (hydration, tautomerization, or cyclization) that convert them to stable products. These stable products are the ones relevant to subsequent polymerization and were considered for this work. Specifically, we considered hydrated quinone methides (β -O4), pinosresinols (β - β), and phenylcoumarans (β -5) (Figure 1D). Initial structures of GG homodimers were obtained from the Cambridge Crystallographic Data Centre (CCDC) and modified using Molden²⁹ to prepare the structures of β -O4, β - β , and β -5 homo- and heterodimers and trimers (hydrated quinone methides). All possible stereoisomers of the dilignols were examined for each of the three linkages. For each stereoisomer, an MM3³⁰ Monte Carlo conformational search was performed to identify low-energy conformers with the *scan* module from the Tinker suite of programs.³¹ Missing force field parameters were assigned by analogy to similar existing parameters. The 25 lowest-energy conformers of each stereoisomer were then optimized with the closed-shell formalism at the B3LYP/6-31+G(d)^{32,33} level of theory with NWChem.³⁴ The lowest-energy conformer of each stereoisomer (e.g., four

Table 1. Comparison of Computed BDEs^a and the Sum of the MO Coefficients for the p Orbitals of the Phenolic Oxygen in the HOMO with EPR-Based Peroxidase Assays from Reference 28

entry	substrate	BDE ^a (kcal/mol)	HOMO energy (eV)	MO coefficient (p_{tot}) ^b	prediction ^c	HRP substrate: ^d
Monomers						
1	H	83.8	-7.33	0.45	yes	yes
2	G	84.0	-7.09	0.45	yes	yes
3	S	80.4	-6.89	0.47	yes	yes
β -O4 Dimers						
4	HH	87.2	-7.48	0.06	no	no
5	GG	85.5	-7.16	0.62	yes	yes
6	HG	86.1	-7.49	0.45	yes	nd
7	GH	86.3	-7.30	0.49	yes	nd
β - β Dimers						
8	HH	85.9	-7.56	0.63	yes	yes
9	GG	85.3	-7.19	0.49	yes	yes
10	GH	85.5	-7.25	0.68	yes	nd
11	HG	86.5	-7.25	0.03	no	nd
β -5 Dimers						
12	HH	86.2	-7.24	0.06	no	no
13	GG	86.0	-7.08	0.02	no	nd
14	HG	86.3	-7.06	0.04	no	nd
15	GH	86.2	-7.27	0.28	no	no
Trimers						
16	HGG(β -5)	89.8	-7.03	0.13	no	nd
17	HGG(β - β)	86.6	-7.26	0.00	no	nd

^aM06-2X/6-311++G(d,p) BDEs at 298 K. ^bHF/STO-3G MO coefficients for the p orbitals of the phenolic oxygen in the HOMO of the lignin precursors. The MO coefficients for the $2p_x$, $2p_y$, and $2p_z$ orbitals were summed to yield p_{tot} . ^cPrediction that a substrate can or cannot undergo oxidation on the basis of the HOMO electron density on the phenolic oxygen. ^dConclusion based on EPR spectra of HRP in the presence of hydrogen peroxide and mono- or dilignols. The appearance of a peak at $g = 6.28$ and corresponding loss of a peak at $g = 2.003$ indicate that the lignin precursor underwent oxidation by HRP. See ref 28 for details; nd = not done.

for β -O4 and two each for β - β and β -5 linkages) was then reoptimized at the M06-2X/6-311++G(d,p)³⁵ level of theory with Gaussian09.³⁶ The single stereoisomer with the lowest energy for each linkage was then used for further analysis. Vibrational frequency calculations and frontier MO analyses were performed at the same level of theory. Solvation effects were approximated by applying the integral equation formalism-polarized continuum model³⁷ (IEF-PCM) to the gas-phase M06-2X/6-311++G(d,p) geometries with water as the solvent. An isovalue of 0.03 was used to plot the highest occupied molecular orbital (HOMO) density maps. To enable simple, qualitative interpretations, MO coefficients were computed at the HF/STO-3G level of theory using M06-2X/6-311++G(d,p) geometries. The qualitative shapes of the orbitals calculated using the two methods are similar (Figures S2 and S3, Supporting Information). Lignin trimers were constructed by manually adding a third monomer unit to the lowest-energy stereoisomer of the corresponding dimers. Conformational analyses and geometry optimizations of the trimers were performed as for the dimers.

RESULTS AND DISCUSSION

To investigate the effects of incorporating monolignol radicals into short lignin chains through the most common interunit linkages found in natural lignin, we first computed the BDEs of the phenolic OH bond in mono- and dilignols. BDEs for homo- and heterodimers comprising H and G subunits, that is, HH, HG, GH, and GG dimers, were calculated (Table 1). For heterodimers with a given interunit linkage, the two subunits can be linked in two different ways. For example, a β -O4 dilignol composed of H and G subunits can be linked between

C_β of the H subunit and O4 of G to form an HG dilignol, or vice versa to form a GH dilignol. In the case of β - β heterodimers, both reaction sites are C_β ; therefore, HG and GH dilignols are identical. β - β dilignols have two phenolic groups available for radical formation, and the BDEs for the two corresponding phenolic O-H bonds in the β - β HG dilignol are expected to be different; therefore, both were considered. β -O4 and β -5 dilignols have a single, free phenolic group.

The BDE is defined as the difference in total energy (including zero-point energy corrections) of the neutral phenol and its homolytic dissociation products according to the reaction



where R-OH is a mono-, di-, or trilignol. BDEs have been considered previously in the context of substituent effects on the ability of phenols to undergo oxidation and act as radical scavengers in biological systems^{38,39} and were found to correlate well with the radical formation capacity of phenols with electron-donating or electron-withdrawing substituents at the meta and para positions.⁴⁰

The computed BDEs for H and G monolignols are 83.8 and 84.0 kcal/mol, respectively (Table 1). The BDE for the S monolignol is somewhat lower at 80.4 kcal/mol due to stabilization of the radical by the two electron-donating methoxy groups ortho to the phenolic oxygen. The BDEs for H and G homo- and heterodimers are slightly higher than those for the H and G monomers, by ~ 1.6 – 3.4 kcal/mol, respectively (Table 1). Hence, the BDEs suggest that, in general, it is more difficult to form phenoxy radicals from dilignols than from monolignols. This difference is to be expected due to the

greater delocalization of spin, and correspondingly greater stability, in the monomer-derived radicals. That is, in the monolignol radicals, spin density is delocalized over the aromatic ring and the vinyl group (Figure S1, Supporting Information), whereas in the dilignol radicals, the spin density is restricted to the aromatic ring because the $C_{\alpha}-C_{\beta}$ double bond is saturated.

The ability of various lignin precursors to undergo peroxidase-catalyzed oxidation has been investigated previously using EPR spectroscopy.²⁸ Several trends are evident in those findings (Table 1). First, monolignols are better substrates than dilignols. Second, an increased number of methoxy substituents (i.e., going from H to G or S) in the mono- and dilignols correlated with increased reactivity as substrates. Third, whereas dilignols with β -O4 or β - β linkages underwent oxidation to various extents by HRP, those with β -5 linkages did not.

These results can be rationalized in part on the basis of BDE if it is assumed that a higher BDE will lead to more sluggish oxidation. For example, the greater reactivity of monolignols than dilignols toward oxidation by HRP is consistent with this idea, as is the greater reactivity of the β -O4 GG dimer in comparison to the HH dimer, which is essentially unreactive. However, certain observations cannot be rationalized on the basis of BDE alone. In particular, the BDEs for the reactive β - β homodimers (entries 8 and 9, Table 1) are very close (within ~ 1 kcal/mol) to those of the unreactive β -O4 HH (entry 4) β -5 HH and β -5 GH dilignols. Thus, for the dilignols, the computed BDEs clearly do not distinguish between experimentally good and poor substrates.

Given the lack of predictive power in the BDE, we sought alternative explanations for the observed selectivity in the enzymatic oxidation. The fundamental problem with BDE as a predictive tool is that it provides information only about the overall thermodynamic favorability of radical formation. The BDE relates clearly to the expected reactivity for roughly thermoneutral hydrogen-atom-transfer reactions but not necessarily toward other pathways leading to phenolic radicals. In lignin polymerization, the oxidizing species is an enzyme, for which HRP is a model. It is believed that HRP and other enzymatic oxidants use a proton-coupled electron transfer (PCET) mechanism to oxidize lignin precursors.⁴¹ In a PCET reaction, an electron and a proton are transferred in a concerted manner to the active site of the enzyme, resulting in net homolysis of the phenolic O-H bond in a lignin precursor. For such a reaction, chemical factors that govern the ease of electron donation, in particular, the energy and structure of the HOMO, are expected to be important determinants of the activation energy. For rapid electron transfer, the HOMO should have both an energy similar to the LUMO of the enzyme and appreciable electron density localized on the phenolic oxygen. If there is a large energy mismatch or weak HOMO electron density on the phenolic oxygen, then electron transfer from the substrate to the enzyme will be slow. These considerations led us to perform MO analyses of mono-, di-, and trimeric lignin precursors to examine in detail the underlying factors that determine their suitability for endwise polymerization. We considered specifically the energy of the HOMO and the p orbital HOMO electron density of the phenolic oxygen undergoing oxidation.

We first considered the HOMO energy of lignin precursors as it has been shown previously that a correlation exists between the HOMO energy and the oxidation rate of simple

phenols and anilines by HRP, with an increase in HOMO energy leading to a higher oxidation rate constant.⁴² The same rule might therefore be expected to hold for phenolic lignin precursors. However, HOMO energies do not obviously correlate with the oxidation rate of some of the dilignols studied here (Table 1). For example, the oxidation of β -5 (entry 12) and β -O4 (entry 4) HH dilignols, with HOMO energies of -7.24 and -7.48 eV, respectively, would, according to this criterion, be more favorable than that for the β - β HH dilignol (entry 8), which has a lower HOMO energy of -7.56 eV. However, both the β -5 and the β -O4 HH dilignols are poor peroxidase substrates, whereas the β - β HH dilignol is a better one.²⁸ Thus, HOMO energies alone do not reliably predict the tendency of lignin precursors to undergo oxidation.

Next, we investigated the structure of the HOMO in lignin precursors, in particular, the p orbital density at the phenolic oxygen. Figure 2 depicts the calculated HOMOs for the three

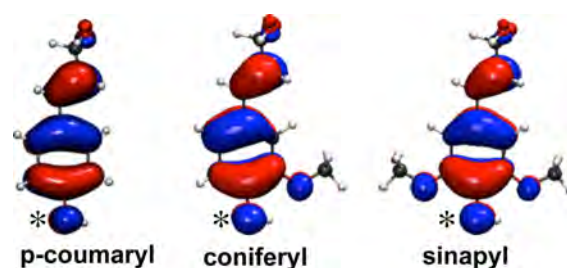


Figure 2. HOMO density plots for monolignols. Phenolic oxygens are indicated by an asterisk.

monolignols. For each molecule, the HOMO density plots are similar and clearly show the presence of strong electron density on the phenolic oxygens, consistent with the strong p orbital coefficients ($p_{\text{tot}} \geq 0.45$, Table 1), as well as extensive delocalization. In contrast, HOMO orbital density maps for dilignols reveal stark differences among them. In the β -O4-linked dilignols, strong electron density is observed on the phenolic oxygens of all except for the HRP-unreactive HH dilignol (Figure 3). Also conspicuous is the substantial localization of orbital density onto one or the other subunit in several cases.

In the case of the β - β dilignols, there are two potential phenolic OH groups that can undergo oxidation. In HH and GG, the phenolic OH groups on both of the H or G subunits have identical local chemical environments (i.e., H or G environment) and, neglecting stereochemical differences, are chemically equivalent in the ensemble average. Although individual conformers within the ensemble can have non-equivalent oxygens, the minimum-energy dilignol structures in our calculations showed similar p orbital HOMO electron densities on both phenolic oxygens (Figure 3). In contrast, for the GH dilignol (equivalent to HG), the two potential phenolic OH groups are in chemically distinct local environments, with one located on the H subunit and the other on a methoxylated G subunit. In all cases, at least one phenolic oxygen has strong p orbital density. However, in the GH/HG dilignol, the orbital density is localized almost entirely on the G subunit (Table 1, entries 10 and 11). Hence, considerable difference in reactivity is expected at the two distinct phenolic oxygens.

For β -5 dilignols, there is only one phenolic OH group available for oxidation. In general, HOMO analysis shows little or no electron density on the phenolic oxygen in the β -5

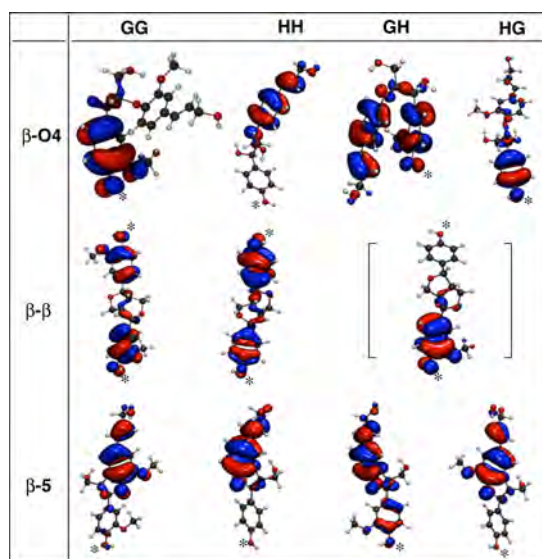


Figure 3. HOMO electron density maps of homo- and heterodimers with β -O4, β - β , and β -5 interunit bonds (top to bottom). The magnitude of the HOMO electron density on the phenolic oxygen correlates with the ability of the compound to undergo oxidation by HRP from a phenolic radical. β - β GH and HG are identical by symmetry. Phenolic oxygens are indicated by an asterisk.

dilignols, in contrast to the β -O4 and β - β dilignols (Figure 3 and Table 1). In the β -5 dilignols, the HOMO orbital density is localized strongly on the nonphenolic subunit containing the intact, conjugated allylic alcohol unit. Of these, two (HH and GH, entries 12 and 15 in Table 1) have been tested with HRP and found to be poor substrates.

In comparing the HOMO energy and structure with the reactivity data from Table 1, certain trends emerge. First, there is no obvious connection between the HOMO energy and reactivity. Second, the HOMO electron density on the phenolic oxygen is a good indicator of reactivity toward HRP. In particular, reactive compounds have a sum of p orbital MO coefficients of $p_{\text{tot}} > 0.4$, but the unreactive have $p_{\text{tot}} < 0.3$. Most of the unreactive compounds have essentially no p orbital density ($p_{\text{tot}} \leq 0.06$). The β -5 GH dimer is particularly interesting because it is near the threshold for reactivity, with a $p_{\text{tot}} = 0.28$. In the other β -5 dilignols, the cinnamyl moiety dominates the HOMO, with strong contributions from the p orbitals of the allylic double bond (Figure 3). Examination of the HOMO density plot for the GH dilignol (Figure 3), however, shows considerable leakage of the orbital density from the cinnamyl alcohol H subunit into the phenolic G subunit. This effect can be understood qualitatively as a consequence of electron donation from the 3-methoxy substituent on the G subunit, which raises the π -energy level on the G subunit to match more closely that of the H subunit and thereby facilitates orbital mixing. Thus, the modest HOMO density on the phenolic oxygen in the β -5 GH dimer is apparently not sufficient for effective oxidation by horseradish peroxidase.

To determine how much the phenolic oxygen HOMO density depends on the conformation of a given dilignol, we computed p_{tot} for a number of low-energy conformers. We considered the β -O4 GG and β - β GH dimers, which are representative of good substrates, and the β -O4 HH and β -5 HH dilignols, which are bad substrates. For the β -O4 GG dimer, computed p_{tot} values varied from 0.43 to 0.65 for the set of 25 low-energy conformers (Table S2, Supporting Informa-

tion). In contrast, p_{tot} for the β -O4 HH dimer was in the range of 0.04–0.18 (Table S3, Supporting Information), the entire span of which is below the apparent threshold for reactivity as peroxidase substrates. For the β - β GH dilignol, which has two available phenolic oxygens, p_{tot} for the G subunit phenolic oxygen was in the range of 0.61–0.72, whereas the values for the phenolic oxygen on the H subunit were between 0.02 and 0.12 (Table S4, Supporting Information). In the case of the β -5 HH dilignol, p_{tot} varied only between 0.04 and 0.05 (Table S5, Supporting Information). Thus, although p_{tot} exhibits some conformational variation for the dimers tested, particularly for the species with greater conformational flexibility, the conformational dependence of p_{tot} is relatively minor and does not alter the conclusions obtained by considering only the lowest-energy conformer identified for each dilignol. That is, the electronic structure is intrinsic to the molecule and is only minimally perturbed by conformational changes.

We also considered the effects of solvation by computing p_{tot} values for gas-phase geometries with the IEF-PCM continuum solvation model with water as the solvent. In general, solvation reduces p_{tot} values slightly relative to the gas-phase values. However, for the β - β GG dimer, p_{tot} increased by 0.07 when solvation effects were included (Table S6, Supporting Information). Interestingly, the reduction of the p_{tot} value for the β -5 GH dilignol from 0.28 in the gas phase to 0.10 in water indicates that perhaps this molecule is not as close to the threshold for reactivity as expected based on the gas-phase value. In summary, solvation effects, at least within the approximations used here, do not alter either the electronic structures of the dilignols or the conclusions made with gas-phase p_{tot} values.

From the trends seen with experimentally tested substrates, we make the following predictions for the untested dilignols (Table 1) on the basis of p_{tot} in the HOMO.

(i) The β -O4 HG and GH dilignols will both be good substrates for HRP and will support lignin elongation.

(ii) The β - β GH/HG dilignol will be oxidized and will support chain elongation only from the G terminus.

(iii) None of the β -5 dilignols will be good substrates or support chain elongation.

To extend our investigation of the effects of linkage and subunit type in lignin polymers further, we considered two HGG trilignols. Because the majority of the interunit bonds in natural lignin are β -O4, the two G subunits in the model trilignols were linked with β -O4 bonds. The terminal H subunit was linked by either a β -5 or β - β bond to obtain the trimeric species (Figure 3). The question thus asked is whether radical formation of this type is also disfavored in the corresponding trilignols. In the HOMO maps for both trilignols, the phenolic oxygen on the H subunit again lacks electron density (Figure 4), and the p_{tot} values (Table 1, entries 16 and 17, respectively) are 0.13 and 0.00. Thus, we expect both of these substrates to be unreactive toward HRP at their H termini despite having relatively high HOMO energies.

CONCLUDING REMARKS

Our findings and the resulting model have important implications for understanding the growth of lignin polymers. Although the factors that control lignin polymerization in vivo are likely to be complex and may include, for example, the availability of substrate, compartmentalization, chemical environment, and enzyme-binding effects, the present work provides evidence that the intrinsic chemical features of lignin

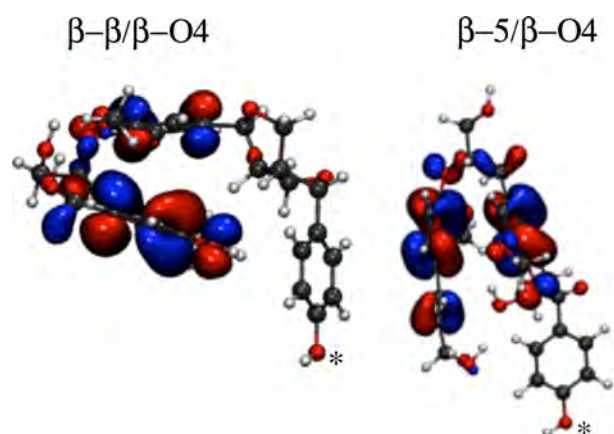


Figure 4. HOMOs of HGG triligols. The lack of HOMO electron density on the phenolic oxygen on the terminal H subunit indicates that phenol radical formation will be unfavorable.

precursors also play an important role. In particular, our findings point to p electron density on the phenolic oxygen as a key determinant of reactivity toward oxidation by HRP or other peroxidases.

Using this criterion, we can rationalize the observation that increasing the relative abundance of the H subunit leads to lignin polymers with reduced molecular weight. A key factor driving this effect is the unreactivity of terminal H subunits in certain common linkages. That is, comparing the expected reactivity of analogous GX and HX pairs ($X = H$ or G), we find that β -O4 GH and β - β GG dilignols are reactive, whereas the corresponding compounds with H termini, that is, β -O4 HH and β - β HG dilignols, are not. Thus, incorporation of H subunits at termini through these linkages slows or stops lignin chain elongation, effectively capping the growing chain at that end. These findings are consistent with observations that the incorporation of a higher percentage of H subunits into G-rich lignin will lead to polymers with shorter chain length and lower molecular weight.⁸ Additionally, the β -5 linkage in general, with either a G or H terminus, is predicted to inhibit elongation. Our findings therefore suggest that a high proportion of H subunits and β -5 linkages might be expected at the termini of lignin polymer chains produced by enzymatic oxidation, though not necessarily those produced by chemical oxidation.

■ ASSOCIATED CONTENT

📄 Supporting Information

Spin density maps of mono- and dilignols, comparisons of HOMO electron density maps and MO coefficients computed at the HF/STO-3G and M06-2X/6-311++G(d,p) levels of theory, HOMO analyses of low-energy conformers of selected dilignols and for the lowest-energy conformer of all mono-, di-, and triligols in continuum solvent, and complete ref 36. This material is available free of charge via the Internet at <http://pubs.acs.org>.

■ AUTHOR INFORMATION

Corresponding Author

*E-mail: parksjm@ornl.gov.

Notes

The authors declare no competing financial interest.

■ ACKNOWLEDGMENTS

The authors thank Ariana Beste and Arthur J. Ragauskas for helpful discussions. This research was supported by the Bioenergy Science Center, which is a U.S. Department of Energy Bioenergy Research Center supported by the office of Biological and Environmental Research in the Department of Energy Office of Science. This work was conducted using the resources at the National Energy Research Scientific Computing Center (NERSC) under Grant Numbers m906 and m1305.

■ REFERENCES

- (1) Ragauskas, A.; Williams, C. K.; Davison, B. H.; Britovsek, G.; Cairney, J.; Eckert, C. A.; Frederick, W. J., Jr.; Hallet, J. P.; Leak, D. J.; Liotta, C. L.; Mielenz, J. R.; Murphy, R.; Templer, R.; Tchapinski, T. The Path Forward for Biofuels and Biomaterials. *Science* **2006**, *311*, 484–489.
- (2) Simmons, B. A.; Loque, D.; Ralph, J. Advances in Modifying Lignin for Enhanced Biofuel Production. *Curr. Opin. Plant Biol.* **2010**, *13*, 312–319.
- (3) Jorgensen, H.; Kristensen, J. B.; Felby, C. Enzymatic Conversion of Lignocellulose into Fermentable Sugars: Challenges and Opportunities. *Biofuels, Bioprod. Biorefin.* **2007**, *1*, 119–134.
- (4) Chapple, C.; Ladisch, M.; Meilan, R. Loosening Lignin's Grip on Biofuel Production. *Nature* **2007**, *25*, 746–748.
- (5) Li, X.; Weng, J.-K.; Chapple, C. Improvement of Biomass through Lignin Modification. *Plant J.* **2008**, *54*, S69–S81.
- (6) Zheng, Y.; Pan, Z.; Zhang, R. Overview of Biomass Pretreatment for Cellulosic Ethanol Production. *Int. J. Agric. Biol. Eng.* **2009**, *2*, 51–68.
- (7) Ding, S.-Y.; Liu, Y.-S.; Zeng, Y.; Himmel, M. E.; Baker, J. O.; Bayer, E. A. How Does Plant Cell Wall Nanoscale Architecture Correlate with Enzymatic Digestibility? *Science* **2012**, *338*, 1055–1060.
- (8) Chundawat, S. P. S.; Beckham, G. T.; Himmel, M. E.; Dale, B. E. Deconstruction of Lignocellulosic Biomass to Fuels and Chemicals. *Annu. Rev. Chem. Biomol. Eng.* **2011**, *2*, 6.1–6.25.
- (9) Himmel, M. E.; Ding, S.-Y.; Johnson, D. K.; William, S. A.; Nimlos, M. R.; Brady, J. W.; Foust, T. D. Biomass Recalcitrance: Engineering Plants and Enzymes for Biofuels Production. *Science* **2007**, *315*, 804–807.
- (10) Himmel, M. E.; Xu, Q.; Luo, Y.; Ding, S.-Y.; Lamed, R.; Bayer, E. A. Microbial Enzyme Systems for Biomass Conversion: Emerging Paradigms. *Biofuels* **2010**, *1*, 323–341.
- (11) Jin, M.; Balan, V.; Gunawan, C.; Dale, B. E. Consolidated Bioprocessing (CBP) Performance of *Clostridium phytofermentans* on AFEX-Treated Corn Stover for Ethanol Production. *Biotechnol. Bioeng.* **2011**, *108*, 1290–1297.
- (12) Beckham, G. T.; Mathews, J. F.; Peters, B.; Bomble, Y. J.; Himmel, M. H.; Crowley, M. F. Molecular Level Origins of Biomass Recalcitrance: Decrystallization Free Energies for Four Common Cellulose Polymorphs. *J. Phys. Chem. B* **2011**, *115*, 4118–4127.
- (13) Fu, C.; Mielenz, J. R.; Xiao, X.; Ge, Y.; Hamilton, C. Y.; Rodriguez, M.; Chen, F.; Foston, M.; Ragauskas, A.; Bouton, J. Genetic Manipulation of Lignin Reduces Recalcitrance and Improves Ethanol Production from Switchgrass. *Proc. Natl. Acad. Sci. U.S.A.* **2011**, *108*, 3803–3808.
- (14) Whetten, R. W.; MacKay, J. J.; Sederoff, R. R. Recent Advances in Understanding Lignin Biosynthesis. *Annu. Rev. Plant Physiol. Plant Mol. Biol.* **1998**, *49*, 585–609.
- (15) Monties, B.; Fukushima, K. *Lignin, Humic Substances and Coal*; Wiley-VCH: Weinheim, Germany, 2001; pp 1–64.
- (16) Ziebell, A.; Gracom, K.; Katahira, R.; Chen, F.; Pu, Y. Q.; Ragauskas, A.; Dixon, R. A.; Davis, M. Increase in 4-Coumaryl Alcohol Units During Lignification in Alfalfa (*Medicago sativa*) Alters the Extractability and Molecular Weight of Lignin. *J. Biol. Chem.* **2010**, *285*, 38961–38968.

- (17) Liu, C.-J. Deciphering the Enigma of Lignification: Precursor Transport, Oxidation and the Topochemistry of Lignin Assembly. *Mol. Plant* **2012**, *5*, 304–317.
- (18) Vanholme, R.; Demedts, B.; Morreel, K.; Ralph, J.; Beorjan, W. Lignin Biosynthesis and Structure. *Plant Physiol.* **2010**, *153*, 895–905.
- (19) Morreel, K.; Ralph, J.; Kim, H.; Lu, F.; Goeminne, G.; Ralph, S.; Messens, E.; Boerjan, W. Profiling of Oligolignols Reveals Monolignol Coupling Conditions in Lignifying Poplar Xylem. *Plant Physiol.* **2004**, *136*, 3537–3549.
- (20) Ralph, J.; Lundquist, K.; Brunow, G.; Lu, F.; Kim, H.; Schatz, P. F.; Marita, J. M.; Hatfield, R. D.; Ralph, S. A.; Christensen, J. H. Lignins: Natural Polymers from Oxidative Coupling of 4-Hydroxyphenylpropanoids. *Phytochem. Rev.* **2004**, *3*, 29–60.
- (21) Brunow, G.; Kilpelainen, I.; Sipila, J.; Syrjanen, K.; Karhunen, P.; Setälä, H.; Rummakko, P. *Oxidative Coupling of Phenols and the Biosynthesis of Lignin*; 1998; Vol. 697, pp 131–147.
- (22) Freudenberg, K. Biosynthesis and Constitution of Lignin. *Nature* **1959**, *183*, 1152–1155.
- (23) Aoyama, W.; Sasaki, S.; Matsumara, S.; Mitsunaga, T.; Hirai, H.; Tsutsumi, Y.; Nishida, T. Sinapyl Alcohol-Specific Peroxidase Isoenzyme Catalyzes the Formation of the Dehydrogenative Polymer from Sinapyl Alcohol. *J. Wood Sci.* **2002**, *48*, 497–504.
- (24) Kobayashi, T.; Taguchi, H.; Shigematsu, M.; Tanahashi, M. Substituent Effects of 3,5-Disubstituted *p*-Coumaryl Alcohols on Their Oxidation Using Horseradish Peroxidase-H₂O₂ as the Oxidant. *J. Wood Sci.* **2005**, *51*, 607–614.
- (25) Mattinen, M.-L.; Surotti, T.; Gosselink, R.; Argyropoulos, D. S.; Evtuguin, D.; Suurnakki, A.; de Jong, E.; Tamminen, T. Polymerization of Different Lignins by Laccase. *BioResources* **2008**, *3*, 549–565.
- (26) Christensen, J. H.; Baucher, M.; O'Connell, A. P.; Van Montagu, M.; Boerjan, W. *Molecular Biology of Woody Plants*; Kluwer Academic Publishers: Dordrecht, The Netherlands, 2000; Vol. 1.
- (27) Sangha, A. K.; Parks, J. M.; Standaert, R. F.; Ziebell, A.; Davis, M.; Smith, J. C. Radical Coupling Reactions in Lignin Synthesis: A Density Functional Theory Study. *J. Phys. Chem. B* **2012**, *116*, 4760–4768.
- (28) Russell, W. R.; Burkitt, M. J.; Scobbie, L.; Chesson, A. EPR Investigation into the Effects of Substrate Structure on Peroxidase-Catalyzed Phenylpropanoid Oxidation. *Biomacromolecules* **2006**, *7*, 268–273.
- (29) Schaftenaar, G.; Noordik, J. H. Molden: A Pre- and Post-Processing Program for Molecular and Electronic Structures. *J. Comput.-Aided Mol. Design* **2000**, *14*, 123–134.
- (30) Allinger, N. L.; Yuh, Y. H.; Lii, J.-H. Molecular Mechanics. The MM3 Force Field for Hydrocarbons. 1. *J. Am. Chem. Soc.* **1989**, *111*, 8551–8566.
- (31) Ponder, J. W.; Richards, F. M. An Efficient Newton-Like Method for Molecular Mechanics Energy Minimization of Large Molecules. *J. Comput. Chem.* **1987**, *8*, 1016–1024.
- (32) Becke, A. D. A Density-Functional Thermochemistry III. The Role of Exact Exchange. *J. Chem. Phys.* **1993**, *98*, 5648–5652.
- (33) Lee, C.; Yang, W.; Parr, R. G. Development of the Colle-Salvetti Correlation-Energy Formula into a Functional of the Electron Density. *Phys. Rev. B* **1988**, *37*, 785–789.
- (34) Valiev, M.; Bylaska, E. J.; Govind, N.; Kowalski, K.; Straatsma, T. P.; van Dam, H. J. J.; Nieplocha, J.; Apra, E.; Windus, T. L.; de Jong, W. A. NWChem: A Comprehensive and Scalable Open-Source Solution for Large Scale Molecular Simulations. *Comput. Phys. Commun.* **2010**, *181*, 1477–1489.
- (35) Chai, J. D.; Head-Gordon, M. Long-Range Corrected Double-Hybrid Density Functionals. *J. Chem. Phys.* **2009**, *131*, 174105–13.
- (36) Frisch, M. J.; Trucks, G. W.; Schlegel, H. B.; Scuseria, G. E.; Robb, M. A.; Cheeseman, J. R.; Scalmani, G.; Barone, V.; Mennucci, B.; Petersson, G. A.; et al. *Gaussian 09*, revision A.2; Gaussian, Inc.: Wallingford, CT, 2009.
- (37) Tomasi, J.; Mennucci, B.; Cammi, R. Quantum Mechanical Continuum Solvation Models. *Chem. Rev.* **2005**, *105*, 2999–3093.
- (38) Leopoldini, M.; Marino, T.; Russo, N.; Toscano, M. Antioxidant Properties of Phenolic Compounds: H-Atom versus Electron Transfer Mechanism. *J. Phys. Chem. A* **2004**, *108*, 4916–4922.
- (39) Nikolic, K. M. Theoretical Study of Phenolic Antioxidant Properties in Reaction with Oxygen-Centered Radicals. *J. Mol. Struct.: THEOCHEM* **2006**, *774*, 95–105.
- (40) Wu, Y.-D.; Lai, D. K. W. A Density Functional Study of Substituent Effects on the O–H and O–CH₃ Bond Dissociation Energies in Phenol and Anisole. *J. Org. Chem.* **1996**, *61*, 7904–7910.
- (41) Derat, E.; Shaik, S. An Efficient Proton-Coupled Electron-Transfer Process during Oxidation of Ferulic Acid by Horseradish Peroxidase: Coming Full Cycle. *J. Am. Chem. Soc.* **2006**, *128*, 13940–13949.
- (42) Sakurada, J.; Sekiguchi, R.; Sato, K.; Hosoya, T. Kinetic and Molecular Orbital Studies of the Rate of Oxidation of Monosubstituted Phenols and Anilines by Horseradish Peroxidase Compound II. *Biochemistry* **1990**, *29*, 4093–4098.